Biosensors and Bioelectronics 100 (2018) 374–381

Contents lists available at ScienceDirect

Biosensors and Bioelectronics

journal homepage: www.elsevier.com/locate/bios

Processable enzyme-hybrid conductive polymer composites for electrochemical biosensing

Yu Liu[a,b], Anthony P.F. Turner[a], Maojun Zhao[b], Wing Cheung Mak[a,*]

[a] Biosensors and Bioelectronics Centre, Department of Physics, Chemistry and Biology, Linköping University, SE-581 83 Linköping, Sweden
[b] College of Science, Sichuan Agricultural University, Yaan 625014, China

ARTICLE INFO

Keywords:
Bio-conductive composite
PEDOT
Microspheres
Bio-interfaces
Glucose biosensor

ABSTRACT

A new approach for the facile fabrication of electrochemical biosensors using a biohybrid conducting polymer was demonstrated using glucose oxidase (GOx) and poly (3, 4-ethylenedioxythiophene) (PEDOT) as a model. The biohybrid conducting polymer was prepared based on a template-assisted chemical polymerisation leading to the formation of PEDOT microspheres (PEDOT-MSs), followed by in-situ deposition of platinum nanoparticles (PtNPs) and electrostatic immobilisation of glucose oxidase (GOx) to form water processable GOx-PtNPs-PEDOT-MSs. The morphology, chemical composition and electrochemical performance of the GOx-PtNPs-PEDOT-MS-based glucose biosensor were characterised using scanning electron microscopy (SEM), energy-dispersive X-ray spectrometry (EDS), Fourier transform infrared (FTIR) spectroscopy, zeta potential and electrochemical measurements, respectively. The biosensor delivered a linear response for glucose over the range 0.1–10 mM (R^2 = 0.9855) with a sensitivity of 116.25 μA mM^{-1} cm^{-2}, and limit of detection of 1.55 μM (3 × SD/sensitivity). The sensitivity of the developed PEDOT-MS based biosensor is significantly higher (2.7 times) than the best reported PEDOT-based glucose biosensor in the literature. The apparent Michaelis–Menten constant (K_m^{app}) of the GOx-PtNPs-PEDOT-MS-based biosensors was calculated as 7.3 mM. Moreover, the biosensor exhibited good storage stability, retaining 97% of its sensitivity after 12 days storage. This new bio-hybrid conducting polymer combines the advantages of micro-structured morphology, compatibility with large-scale manufacturing processes, and intrinsic biocatalytic activity and conductivity, thus demonstrating its potential as a convenient material for printed bioelectronics and sensors.

1. Introduction

The development of portable and rapid electrochemical biosensors to determine metabolites continues to become increasingly important in distributed healthcare (Bandodkar et al., 2016; Sekretaryova et al., 2016; Tricoli et al., 2017). Advanced bio-interface materials are a key factor for the fabrication of electrochemical biosensors with high stability, sensitivity and selectivity at an affordable cost. Recently, many new materials, such as graphene, graphene oxide (Bo et al., 2017), carbon nanotubes (Yang et al., 2015), nanostructured metal oxides (Solanki et al., 2011) and metal nanoparticles (Saei et al., 2013) have been proposed as interface materials for biomolecule immobilisation, and in some cases signal transduction. The advantages of these materials derives mainly from their large surface area to volume ratio for immobilisation of biomolecules. In the case of metal nanoparticles, carbon nanotubes and graphene, these interfacing materials provide addition electro-catalytic and conductivity functions. Interestingly, metal oxide and graphene oxide have recently attracted attention as popular interfacing materials for bioelectronics (Kumar et al., 2015), even though the conductivity and electro-catalytic functions of such oxide-based materials is questionable. The performance of these materials for the development of biosensors can be enhanced by tailoring the properties of the bio-interface to control their morphology and surface functionalisation. The immobilisation of biomolecules onto metal nanoparticle could be easily achieved by metal-thiol chemistry (Xing et al., 2010). However, due to the poor water dispersity of the inorganic and carbon-based materials such as graphene oxide, surfactant or carboxyl and amine functional surfactant is usually added as a surface stabiliser to create an intermediate interface for immobilisation. However, the addition of an insulating surfactant coating layer could affect the conductivity of such materials for bioelectronic applications.

Recently, organic conducting polymers have attracted considerable attention for biomedical device applications due to their intrinsic electronic and ionic conductivity which bridges the gap between electronics and biology by being electronically and ionically conductive (Simon et al., 2016). Thus, ionic signals generated in the biological

* Corresponding author.
E-mail address: wing.cheung.mak@liu.se (W.C. Mak).

http://dx.doi.org/10.1016/j.bios.2017.09.021
Received 24 July 2017; Received in revised form 12 September 2017; Accepted 14 September 2017
Available online 18 September 2017
0956-5663/

system are more readily transduced to electronic signals through the bio-conducting interface. Improving the processability of conducting polymers allow the easy fabrication of electrochemical interfaces for device applications (Vagin et al., 2016; Wannapob et al., 2017). Moreover, organic conducting polymers can be designed with desired physical morphology (Xia et al., 2010; Wannapob et al., 2015) and chemical properties by chemical dopants (Ishiguro et al., 2011; Tourillon and Garnier, 1983), thus enabling the manufacture of flexible, wearable and portable bioelectronics.

Among the different conducting polymers, poly (3, 4-ethylenedioxythiophene) (PEDOT) is one of the most promising materials for bioelectronic application due to its relatively high conductivity, stability and more importantly its organic nature and **good** compatibility with bio-organic molecules such as enzymes compared to other conducting polymers (Kros et al., 2001; Kergoat et al., 2014). However, due to its poor solubility and processability, PEDOT is often combined with PSS to create water soluble PEDOT: PSS (Thomas and Leung, 2014; Luzio et al., 2011). Doping of PSS could interrupt the connection of the PEDOT chains and reduce their electrochemical performance (Alemu et al., 2012). Although water soluble PEDOT: PSS can be used to create conducting polymer thin films, the resulting plannar film lacks morphological advantage having only limited accessible surface compared with processable colloidal interface materials. Therefore, creating a processable micro-structured PEDOT with, for example, a spherical structure with larger active surface, is attractive as new interface material for catalytic and biocatalytic sensor applications. There are few examples reported in the literature for the fabrication of PEDOT particles. This is due to the poor intrinsic properties of EDOT, such as its relatively low efficiency for oxidative polymerisation and relatively low solubility of the EDOT monomer in the absence of surfactants (Han and Armes, 2003; Henderson et al., 2001; Paradee and Sirivat, 2014). The consequent use of polymeric surfactants or non-ionic surfactants and organic solvent has led to a decrease in the conductivity of PEDOT and environmental issues due to the difficulty of removing the insulating surfactants and the toxicity of organic solvent.

We take a step forward by demonstrating the new concept of enzyme-hybrid PEDOT microspheres (PEDOT-MSs) as an advanced processable bio-conducting interface material for the facile fabrication of electrochemical biosensors. The microstructure of PEDOT-MSs provides a larger active conducting surface for intimate immobilisation of enzyme molecules (i.e. glucose oxidase – GOx) to facilitate the signal transduction process. The structural and chemical characteristics of the resulting GOx-PtNPs-PEDOT-MSs were examined by scanning electron microscope (SEM), energy-dispersive X-ray spectrometry (EDS), Fourier transform infrared (FTIR) spectroscopy, particle size and zeta potential analysis. The electrochemical performance of the resulting glucose biosensors was characterised using cyclic voltammetry and amperometry.

2. Experimental

2.1. Materials

Glucose oxidase (GOx), calcium chloride ($CaCl_2$), sodium carbonate (Na_2CO_3), copper (II) perchlorate hexahydrate $Cu(ClO_4)_2{\cdot}6H_2O$, sodium persulfate ($Na_2S_2O_8$), ethylenediaminetetracetic acid (EDTA), ethanol, 2-propanol, 3, 4-ethylenedioxythiophene (EDOT), potassium tetrachloroplatinate(II) (K_2PtCl_4), sodium borohydride ($NaBH_4$) and Nafion were purchased from Sigma-Aldrich (St. Louis, MO, USA) and were used as received. All other chemicals were analytical grade and used without further purification. All solutions were prepared in milli-Q water.

2.2. Preparation of porous calcium carbonate template

Calcium carbonate ($CaCO_3$) template particles were synthesised by a previously reported method with minor modifications (Volodkin et al., 2010; Sukhorukov et al., 2004; Mak et al., 2010). Briefly, 2 mL of 1 M Na_2CO_3 solution was mixed with an equal volume of 1 M $CaCl_2$ solution in a small beaker with stirring at 80 g for 1 min. The mixed solution turned opaque almost instantly. Then, the $CaCO_3$ microparticles were repeatedly washed by centrifugation (130*g*, 1 min) with water and ethanol twice, followed by washing with 2-propanol. The $CaCO_3$ microparticles obtained were stored in 2-propanol (100 mg mL^{-1}) for further use.

2.3. Preparation poly (3, 4-ethylenedioxythiophene) microspheres (PEDOT-MSs)

A typical preparation process consisted of two key steps: mild oxidation and advanced oxidation. In the mild oxidation step, a primary framework of conducting polymer is formed, which was accompanied by a slow outward diffusion of the monomer from the $CaCO_3$ template occurring simultaneously, leading to insufficient polymer density within the microspheres. This was followed by an advanced oxidation step, by replenishing new monomers within the template and allowing further polymerisation to reinforce the pre-existing polymer network and forming a stable microsphere structure. The detailed experimental process is as follows: For the mild oxidation step: 200 μL of pure EDOT monomer were mixed with 50 mg of $CaCO_3$ microparticles (collected from 500 μL 100 mg mL^{-1} stock $CaCO_3$ microparticles suspension by centrifugation) and incubated for 2 h to allow infusion of the EDOT into the pores of the $CaCO_3$ template particles. After that, the EDOT-loaded $CaCO_3$ microparticles were washed with 2-propanol by centrifugation (130*g*, 1 min) and the excess EDOT was discarded. For polymerisation of EDOT, a mixture composed of 500 μL $Na_2S_2O_8$ (0.2 M) and 120 μL $Cu(ClO_4)_2$ (0.5 M) added to the EDOT-loaded $CaCO_3$ microparticles. The mixture was incubated for 6 h at room temperature (22 °C). The reaction mixture was collected and centrifuged at 130*g* for 2 min, and then the pellet was resuspended and washed twice in 2-propanol, ethanol, milli-Q water and 2-propanol, to produce the pre-matured microparticles. For the advanced oxidation step: the pre-matured microparticles were mixed again with 200 μL of pure EDOT monomer, and incubated for 4 h to allow a deep infusion of the monomers through the partially polymerised network into the interior of the $CaCO_3$ microparticles. Then, the microparticles were washed by centrifugation (130*g*, 1 min) with 2-propanol, followed by addition of the same amount of oxidant as described in the first step to initiate the advanced oxidation process for 24 h at room temperature (22 °C). Then, the microparticle mixture was washed by centrifugation (130*g*, 1 min) with 2-propanol, ethanol and milli-Q water. Subsequently, the PEDOT-$CaCO_3$ microparticles were treated with 1 mL EDTA (0.2 M) for 1 h at room temperature (22 °C) to remove the $CaCO_3$ template. The PEDOT-MSs obtained were washed with 1 mL of milli-Q water three times by centrifugation (130*g*, 1 min) and re-dispersion cycles to remove the EDTA residual. The pure PEDOT-MSs were dried in vacuum chamber for 48 h, then re-dispersed in water to obtain a PEDOT-MSs colloids with concentration of 10 mg mL^{-1} and stored at room temperature for further characterisation.

2.4. Preparation of PtNPs-PEDOT-MSs composite

The PEDOT-MSs (20 μL, 10 mg mL^{-1}, in water) were mixed with K_2PtCl_4 (100 μL, 50 mM) and incubated for 2 h at room temperature allow the absorption of $PtCl_4^{2-}$. Then, 20 μL of $NaBH_4$ (300 mM) was introduced as reductant for the in-situ reduction of platinum ions leading the formation of platinum nanoparticles (PtNPs) on the surface of the PEDOT-MSs. The PtNPs-PEDOT-MSs were collected and washed with water by centrifugation (130*g*, 1 min) to remove the residual reagent and stored in PBS (10 mM, pH 7.4) at concentration of 10 mg mL^{-1}.

2.5. Preparation of GOx-PtNPs-PEDOT-MSs composite

For preparation of GOx-PtNPs-PEDOT-MS composite, 20 μL PtNPs-PEDOT-MSs was mixed with 20 μL glucose oxidase (GOx) (10 mg mL^{-1}) and incubated for 12 h at 4 °C. Finally, the GOx-PtNPs-PEDOT-MSs were washed by PBS (10 mM, pH 7.4),collected by centrifugation (130*g*, 1 min) and stored in 20 μL PBS (10 mM, pH 7.4). The absorption capacity of GOx was determined by measuring the initial enzyme concentration and remaining un-adsorbed enzyme in the supernatant. A standard curve was obtained from a series of standard concentration of GOx solution. The amount of un-adsorbed free enzyme which was collected from supernatant solution was calculated according to a standard curve. In each run, a constant amount of PtNPs-PEDOT-MSs (10 mg mL^{-1}) was used with respect to the different concentration of glucose oxidase (from 2.5 to 15 mg mL^{-1}).

2.6. Electrochemical measurements of the GOx-PtNPs-PEDOT-MSs biosensors

Glucose biosensors were fabricated by direct drop casting of 4 μL of the GOx-PtNPs-PEDOT-MS suspension (10 mg mL^{-1}) on the screen-printed carbon electrodes and drying at room temperature for 4 h, followed by deposition of 2 μL of 0.05 wt% Nafion solution for packaging and protection of the electrode surface. All electrochemical measurements were performed with a PGSTAT30 potentiostat (Autolab, Nertherlands) and the data were analysed using the NOVA or GPES software. The screen-printed electrodes (DS110) were used as supporting electrodes for the fabrication of glucose biosensors. Cyclic voltammetry of different modified electrodes was performed with a potential window of − 0.2 to 0.6 V at a scan rate of 50 mV s^{-1} in PBS (10 mM, pH 7.4). All amperometric measurements were carried out at an applied potential of 0.6 V in PBS (10 mM, pH 7.4).

2.7. Characterisations

Scanning electron microscopy (SEM) images were recorded with a LEO 155 Gemini (Zeiss, OR, USA). The same field of view was then scanned using an energy-dispersive X-ray spectrometer (EDS) to acquire a set of X-ray maps for C, S, O, N and Pt. All microspheres samples suspended in Milli-Q water were applied on a flat silicon surface, air-dried at ambient temperature. The particle size and zeta potentials (surface charge) were measured using a Zetasizer Nano ZS90 (Malvern Instruments Ltd., Worcestershire, U.K.). Fourier transform infrared (FTIR) spectroscopy was performed with VERTEX 70 (Bruker, USA) equipped with a germanium attenuated total reflectance (ATR) sample cell. Spectrophotometric measurements were performed with a NanoDrop ND-1000(Thermo) in the range of 250–700 nm.

3. Results and discussion

Scheme 1 represents the overall process for the preparation of water processable bio-conductive GOx-PtNP-PEDOT-MS composite. The synthesis strategy is firstly to obtain processable PEDOT microspheres by using $CaCO_3$ template-assisted polymerisation under chemical oxidation. This is one of the crucial steps to obtain a water-processable PEDOT that provides a more compatible interface for the attachment of biomolecules (i.e. enzymes) for the preparation of the GOx-PtNPs-PEDOT-MSs composite. PEDOT has a poor solubility and processability. We overcame this limitation by using colloidal chemistry to fabricate polymer materials in the form of microspheres and thus opening up an easy way towards solution-processable materials. The water-processable PEDOT allows the dispersion of PEDOT-MSs in water thus facilitating the conjugation/immoblisation of the water-soluble enzyme (i.e. GOx), which is significant for the preparation of enzyme-hybrid conducting polymer in a biocompatible aqueous environment to maintain the biological activity of the enzyme (Vasilevaa and Godjevargova, 2005). This was followed by the in-situ formation of the PtNPs onto the PEDOT-MSs surface and the enzyme absorption process to obtain the bio-conductive GOx-PtNPs-PEDOT-MSs composite. Despite the fact that both PtNPs and PEDOTs are conducting, they served different functions. PtNPs mainly provided a hydrogen peroxide oxidation catalyst for the detection of glucose based on the GOx reaction, while the processable PEDOT-MSs served as a high surface area micro-structured conducting support for the deposition of the nano-structured PtNPs. Metal nanoparticles have been widely explored for the construction of high-performance electrochemical sensing interfaces because of their excellent catalytic performance. (Liu et al., 2017; Prakash et al., 2013; Lu et al., 2008). Therefore, the PEDOT-MS support could allow a higher loading of PtNPs to be deposited compared to direct deposition of PtNPs onto a plannar electrode surface.

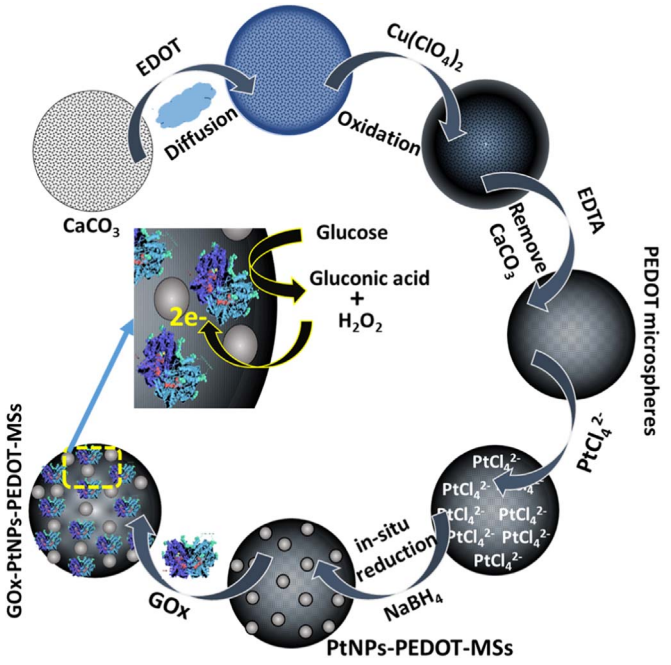

Scheme 1. Schematic representation of the GOx-PtNPs-PEDOT-MSs biohybrid conducting polymer composite.

3.1. Morphological characterisation of the PEDOT-MSs-based composites

Fig. 1 shows the SEM images of (a) PEDOT-MSs, (b) PtNP-PEDOT-MSs and (c) GOx-PtNPs-PEDOT-MSs, respectively. Fig. 1**a** shows that the PEDOT-MSs have an intact spherical morphology with a rough surface and a network of granulated structures. The formation of the granulated structure is likely due to the porous structure of the $CaCO_3$ template that consists of an inorganic crystalised structure with interconnected pores (Achlioptas et al., 2009). The granular structure and the rough surface could further increase the effective surface area of the PEDOT for engrafting of nanomaterials (i.e. PtNPs) and biomolecules (i.e. GOx). The SEM image of PtNPs-PEDOT-MSs is shown in Fig. 1**b**; abundant PtNPs are uniformly distributed on the PEDOT-MS's surface with a diameter of around 55 nm. These well anchored PtNPs will act as the catalytic site for detection of the hydrogen peroxide that is generated from the GOx enzymatic reaction. After absorption of GOx molecules, images of the GOx-PtNPs-PEDOT-MSs (Fig. 1**c**) exhibit a slightly blurry surface due to the electrostatic adsorption of insulating GOx molecules, while the PtNPs remained stable on the PEDOT-MS's surface. Fig. 1**d** shows the size distribution curve of the PEDOT-MSs with an average diameter of 3.18 ± 0.52 μm. The narrow size distribution of the PEDOT-MSs demonstrates the advantage of the $CaCO_3$ templating method for the fabrication of conducting polymer-based materials with

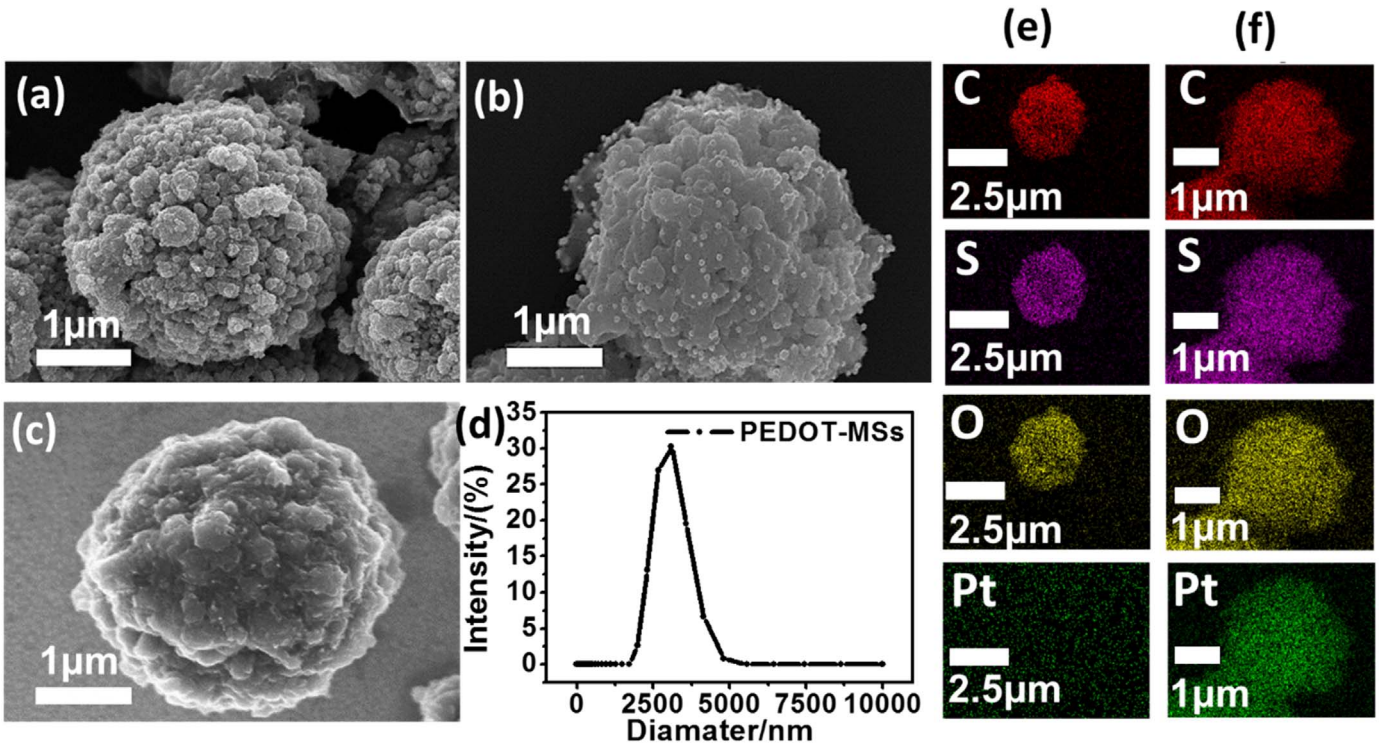

Fig. 1. SEM images of (a) PEDOT-MSs, (b) PtNPs-PEDOT-MSs and (c) GOx-PtNPs-PEDOT-MSs, respectively. (d) Size distribution curve of PEDOT-MSs. EDS maps of (e) PEDOT-MSs and (f) PtNPs-PEDOT-MSs, respectively.

well-defined size and morphology. EDX analysis was performed to characterise the elemental composition of the PEDOT-MSs and PtNP-PEDOT-MSs (Fig. 1**e–f**). A characteristic sulphur peak and oxygen peak were observed for the PEDOT-MSs originating from the EDOT monomer. While, a characteristic platinum peak was observed for the PtNPs-PEDOT-MSs, indicating the successful in-situ formation of PtNPs on the PEDOT-MS's surface.

3.2. Spectroscopic characterisation, zeta potential and water dispersity of the PEDOT-MSs-based composites

The FTIR spectra of synthesised PEDOT-MSs, PtNP-PEDOT-MSs, GOx-PEDOT-MSs and GOx-PtNPs-PEDOT-MSs are presented in Fig. 2**a**. The absorption bands of PEDOT-MSs at 1323, 1192 and 1060 cm^{-1} originated from C-C, C=C, C-O-R-O-C stretching, and the absorption bands at 981, 843, and 687 cm^{-1} corresponded to the vibrations from C–S bonds in the thiophene ring structure (Du et al., 2009). The characteristic band around 750 cm^{-1}, is attributed to the C-H out-of-plane bending vibration at α-α′positions of EDOT, and totally disappeared after polymerisation, thus demonstrating that the EDOT polymerisation was successful. The spectra obtained are in good agreement with those previously reported in literature (Guo et al., 2012; Zhang et al., 2014). In addition, there are no significant differences between the FITR spectrum of the PEDOT-MSs, PtNPs-PEDOT-MSs, GOx-PEDOT-MSs and GOx-PtNPs-PEDOT-MSs. The FTIR results demonstrate that their chemical structure was not affected by the subsequent processes, including the reduction reaction of PtNPs and the enzyme adsorption. Moreover, the chemical polymerisation reaction will produce PEDOT-MSs in an oxidised (conductive) form, which is important for creating a conductive structure for biosensor applications. The surface charge of PEDOT-MSs, PtNPs-PEDOT-MSs, GOx-PEDOT-MSs and GOx-PtNPs-PEDOT-MSs were characterised by zeta potential measurements in PBS at pH 7.4, respectively (Fig. 2**b**). Zeta potential values of pristine PEDOT-MSs, PtNPs-PEDOT-MSs, GOx-PEDOT-MSs and GOx-PtNPs-PEDOT-MSs were 15.03 ± 0.15 mV, − 5.62 ± 0.84 mV, − 13.33 ± 0.64 mV and − 18.87 ± 1.45 mV, respectively. The pristine PEDOT-MSs had a positive zeta potential as a result of the positively charged PEDOT backbone (Dimitriev et al., 2011). While, the PtNPs-PEDOT-MSs had a slightly negatively zeta potential due to the in-situ formation of the negatively charged borohydride-capped PtNPs (Solomon et al., 2007). After adsorption of GOx, the zeta potential values of the resulting GOx-PEDOT-MSs and GOx-PtNPs-PEDOT-MSs were reversed to negatively charge. This could be explained by the fact that GOx has an isoelectric point at pH 4.2. Since the zeta potential measurements were performed at pH 7.4, which is above the isoelectric value of GOx, this leads to the protonation of the GOx molecules and results in a negative surface charge for the GOx-PEDOT-MSs. The observed reverse in surface zeta potential indicates the successful adsorption of the GOx onto the PEDOT-MSs. The adsorption process is likely resulting from the strong interaction between the positively charged PEDOT-MSs and the negatively charged GOx molecules facilitating the formation of stable GOx-PEDOT-MS composites via electrostatic interaction. In order to intuitively observe the dispersity of the PEDOT-MSs in both aqueous suspension and deposited dry film, a suspension of the PEDOT-MSs was allowed to set for 2 h to record the colloidal stability, followed by depositing a droplet of the PEDOT-MSs suspension onto a glass surface and examining the morphology of the dried film (Fig. 2**c**). The optical photographs clearly show that the PEDOT-MSs suspension in water medium remains stable as a homogeneous black coloured solution, which is indicative of the microspheres' good dispersity and colloidal stability. Moreover, the dried PEDOT-MSs film appeared as a homogenous coating layer. This indicates its potential application as a processable material for printed electronics. In contrast, the random-structured PEDOT prepared in the absence of the $CaCO_3$ template, had poor dispersity and significant aggregation, likely due to the high surface roughness of the random structure causing particle aggregation. More importantly, the particle aggregation would greatly restrict the analyte diffusion efficiency and affect the resulting biosensor performance.

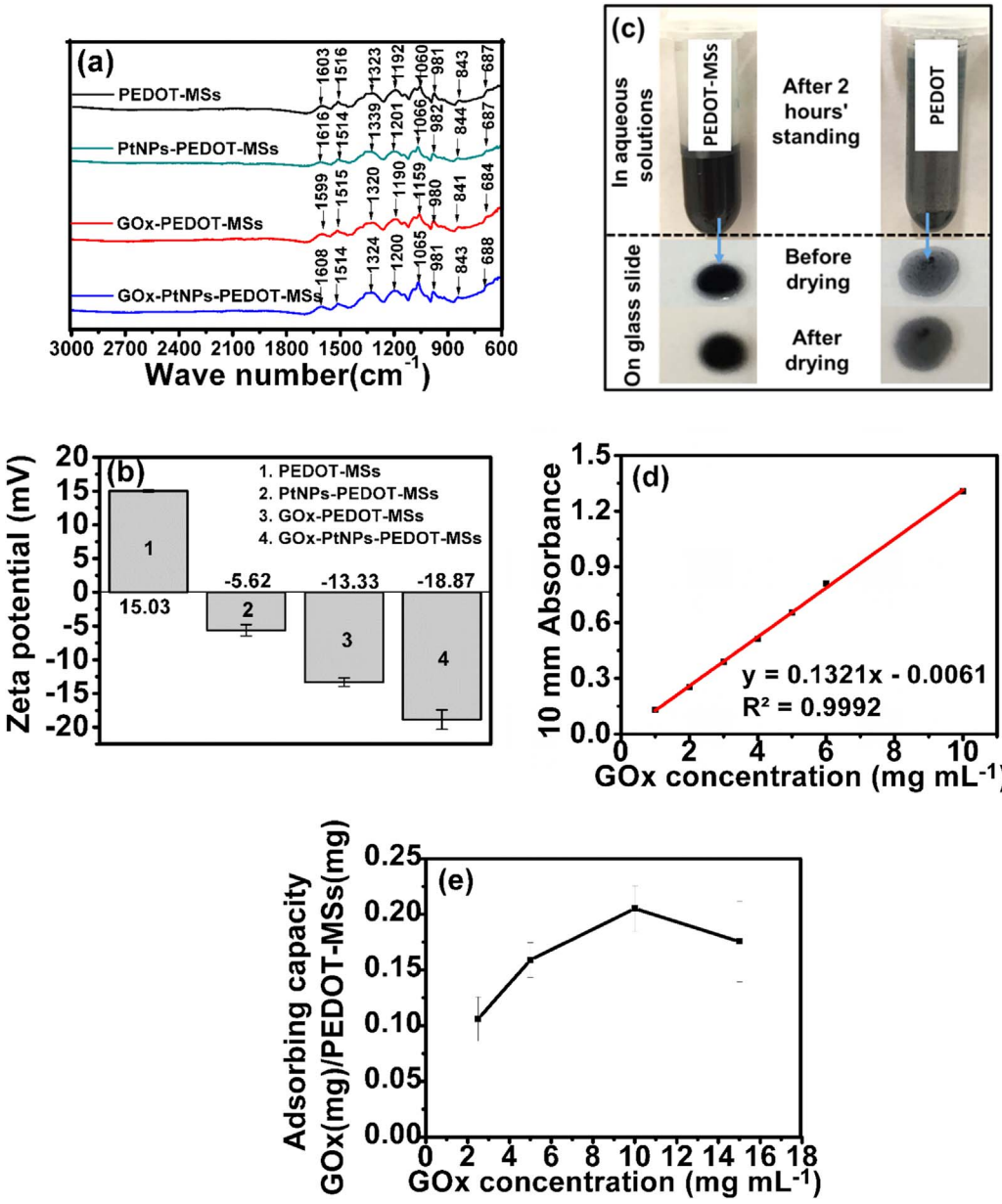

Fig. 2. (a) FTIR spectra and (b) zeta potentials of PEDOT-MSs, PtNPs-PEDOT-MSs, GOx-PEDOT-MSs and GOx-PtNPs-PEDOT-MSs, respectively. (c) Optical photographs showing the dispensability of PEDOT-MSs and PEDOT in water before drying and after drying. (d) Spectrophotometric calibration curve for glucose oxidase based on spectrophotometric. (e) The enzyme absorption capacity of PEDOT-MSs as a function of GOx concentration.

3.3. Enzyme loading capacity of the GOx-PtNPs-PEDOT-MSs

The enzyme loading capacity of the GOx-PtNPs-PEDOT-MSs was determined by spectrophotometric measurement at 280 nm (Mak et al., 2005). After the enzyme adsorption, the GOx-PtNPs-PEDOT-MSs were collected by centrifugation. The initial GOx concentration and the GOx remaining in the supernatant were quantified by UV absorption at 280 nm. The difference in the amount of GOx before and after the adsorption process was calculated and represented the enzyme loading capacity. Fig. 2**d** shows the standard curve of GOx solution over a concentration range from 1 to 10 mg mL^{-1} with a linear equation of $y = 0.1321x - 0.0061$ and correlation coefficient $R^2 = 0.9992$. The enzyme loading studies were performed by incubating the PtNPs-PEDOT-MSs with GOx solution with concentrations ranging from 2.5 to 15 mg mL^{-1} (Fig. 2**e**). The maximum enzyme loading of 0.205 ± 0.02 mg GOx per mg PEDOT-MSs was achieved by using 10 mg mL^{-1} GOx solution.

3.4. Electrochemical properties of the GOx-PtNPs-PEDOT-MSs electrode

The interfacial electrochemical properties of different PEDOT-MSs-based electrodes were characterised by measuring voltammetric responses in 0.1 M PBS solutions containing 5 mM $[Fe(CN)_6]^{3-/4-}$ and 0.1 M KCl. In order to characterise the electrochemical behaviour of the prepared electrode, the redox reaction of $[Fe(CN)_6]^{3-}$ and $[Fe(CN)_6]^{4-}$ was measured for the determination of electron transfer rate by a well-known method of CV analysis (Unnikrishnan et al., 2013). As shown in Fig. 3**a**, all the modified electrodes displayed a pair of typical redox peaks with different peak-to-peak potential separations. Generally, the smaller peak separation indicates fast electron transfer kinetics (Nugent et al., 2001). The peak-to-peak potential separations (ΔEp) for all electrodes were, in order, Nafion/bare SPE (120 mV), Nafion/PEDOT-MSs/SPE (116 mV), Nafion/PtNPs-PEDOT-MSs/SPE (105 mV), Nafion/GOx-PEDOT-MSs/SPE (171 mV), and Nafion/GOx-PtNPs-PEDOT-MSs/SPE (151 mV). It is clear that the Nafion/PEDOT-MSs/SPE and the Nafion/PtNPs-PEDOT-MSs/SPE showed a smaller ΔEp value compared with the bare electrode, indicating a faster electron transfer rate. This indicated that the PEDOT-MSs facilitate faster electron transfer likely

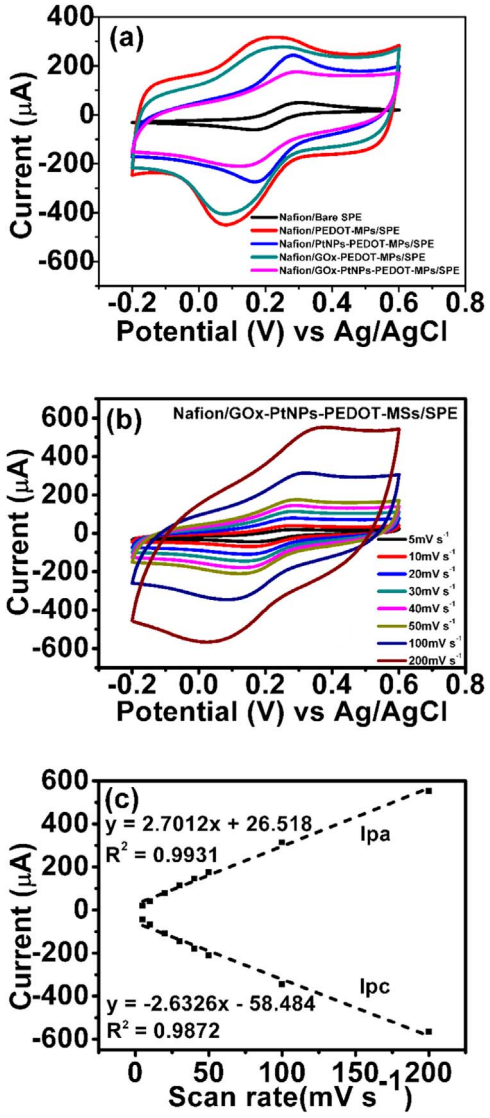

Fig. 3. Cyclic voltammograms of (a) bare and modified electrodes at 50 mV s^{-1} and (b) Nafion/GOx-PtNPs-PEDOT-MSs electrode at various scan rates from 5 to 200 mV s^{-1} in 0.1 M PBS solutions containing 5 mM $[Fe(CN)_6]^{3-/4-}$ and 0.1 M KCl. (c) Plot of I_{pa} and I_{pc} versus scan rates.

due to their large effective surface area and high electrical conductivity. Moreover, when using the PtNPs-PEDOT-MSs, the peak separation further decreased, demonstrating that the introduction of PtNPs further enhanced the electron transfer kinetics. After coupling with the enzyme molecules, both the GOx-PEDOT-MSs and GOx-PtNPs-PEDOT-MSs showed a slight increase in the ΔEp values due to the insulating properties of the enzyme molecules. The observed increase in ΔEp values provide additional evidence for the successful coupling of GOx onto the PEDOT-MSs. The effect of scan rates on the cathodic (I_{pc}) and anodic peaks (I_{pa}) of Nafion/GOx-PtNPs-PEDOT-MSs electrodes is shown in Fig. 3**b**. Both cathodic and anodic peak currents increased with increasing scan rates from 5 to 100 mV s^{-1}, and the linear dependence of the Ipa and the Ipc on scan rate is given in Fig. 3**c**. The linear regression equations for the redox process are: $I_{pa} = 2.7012\nu + 26.518$, $R^2 = 0.9931$; and $I_{pc} = -2.6326\nu - 58.484$, $R^2 = 0.9872$, where, ν is the scan rate. The good correlation coefficient suggests a typical diffusion controlled electrode process.

3.5. GOx-PtNPs-PEDOT-MSs for electrochemical glucose biosensors

The resulting processable bio-conducting GOx-PtNPs-PEDOT-MSs composite was used for the fabrication of electrochemical glucose biosensors using a simple single-step deposition process. The amperometric response of GOx-PtNPs-PEDOT-MSs/SPE was obtained by successively injecting 0.1–30 mM glucose solution and is shown in Fig. 4**a.** Inset is a magnification of the response current with glucose concentration from 0.1 to 1 mM, which showed a good signal response for successive additions of relatively low concentrations of glucose. Calibration curves for glucose were obtained by adding successive aliquots of increasing concentrations of glucose and measuring the steady-state signal responses, which was achieved after around 6 s, as shown in Fig. 4**b**. The calibration curve was linear from 0.1 to 10 mM glucose. The sensitivity and limit of detection were calculated as 116.25 μA mM^{-1} cm^{-2} and 1.55 μM (3 × SD/sensitivity), respectively. It is important to note that the results were obtained from 3 individually prepared biosensors (n = 3). Comparisons of the analytical performance of PEDOT-based glucose biosensors with values found in the literature are shown in Table 1. The sensitivity of the developed PEDOT-MS based biosensor is significantly higher than previously reported PEDOT-based glucose biosensors (Table 1). The high analytical sensitivity could be explained by the morphological properties of the GOx-PtNPs-PEDOT-MS film that has a relatively large active surface and extensive inter-particle space, formed during the particle assembly process, which can facilitate the diffusion of substances (e.g., analytes, electrolytes, etc.) and enhance the performance of the biosensors (Ndamanisha and Guo, 2012; Wu et al., 2007). The standard derivation between measurements is relatively large, likely due to the manual drop casting procedure causing variation in the microparticle film thickness and surface roughness between different individually prepared biosensors (n = 3). However, this could be improved in future by using an automatic deposition system for more precise fabrication of the biosensors.

As shown in Fig. 4**b** the response current increased linearly with increase in glucose concentration at first, and then reached an approximate saturation value at high glucose concentrations beyond 15 mM. This is a typical reflection of Michaelis-Menten kinetics which describes the interaction between the enzyme and substrate. The apparent Michaelis-Menten constant (K_m^{app}) was calculated using a Lineweaver–Burk plot according to the following equation:

$$(1/I) = (K_m^{app}/I_{max})(1/C) + (1/I_{max}).$$

Where I represents the steady-state current after addition of glucose. The maximum current (I_{max}) was determined at saturated level of glucose, and C is the concentration of glucose. The values of I_{max} and K_m^{app} were calculated by the analysis of the intercept and the slope of the plot (Fig. 4**c**). The K_m^{app} value obtained here is 7.3 mM, which is much smaller than that reported in the literature for previous PEDOT-based glucose biosensors: 17.27 mM for GOx entrapped in PEDOT film (Nien et al., 2006), 33 mM for PEG-GOx/PEDOT film (Piro et al., 2001). The relatively small K_m^{app} value could be explained by the intimate coupling of the GOx onto a relatively larger active surface of the PtNPs-PEDOT-MSs (i.e. larger surface-area-to-volume ratio) compared with the reported electrochemical polymerised bulk PEDOT films and the consequent diffusion barrier presented by these systems. Moreover, the unique water processable characteristic of the GOx-PtNPs-PEDOT-MS composite allows the dispersion of the bio-conductive ink in a biomolecule-friendly aqueous environment for the preparation of the bioelectrode and compatibility with large-scale manufacturing processes such as screen-printing, ink-jet printing and drop-on-delivery systems.

3.6. Stability and selectivity of the Nafion/GOx-PtNP-PEDOT-MS/SPE bioelectrode

To investigate the stability of the glucose biosensor, the signal

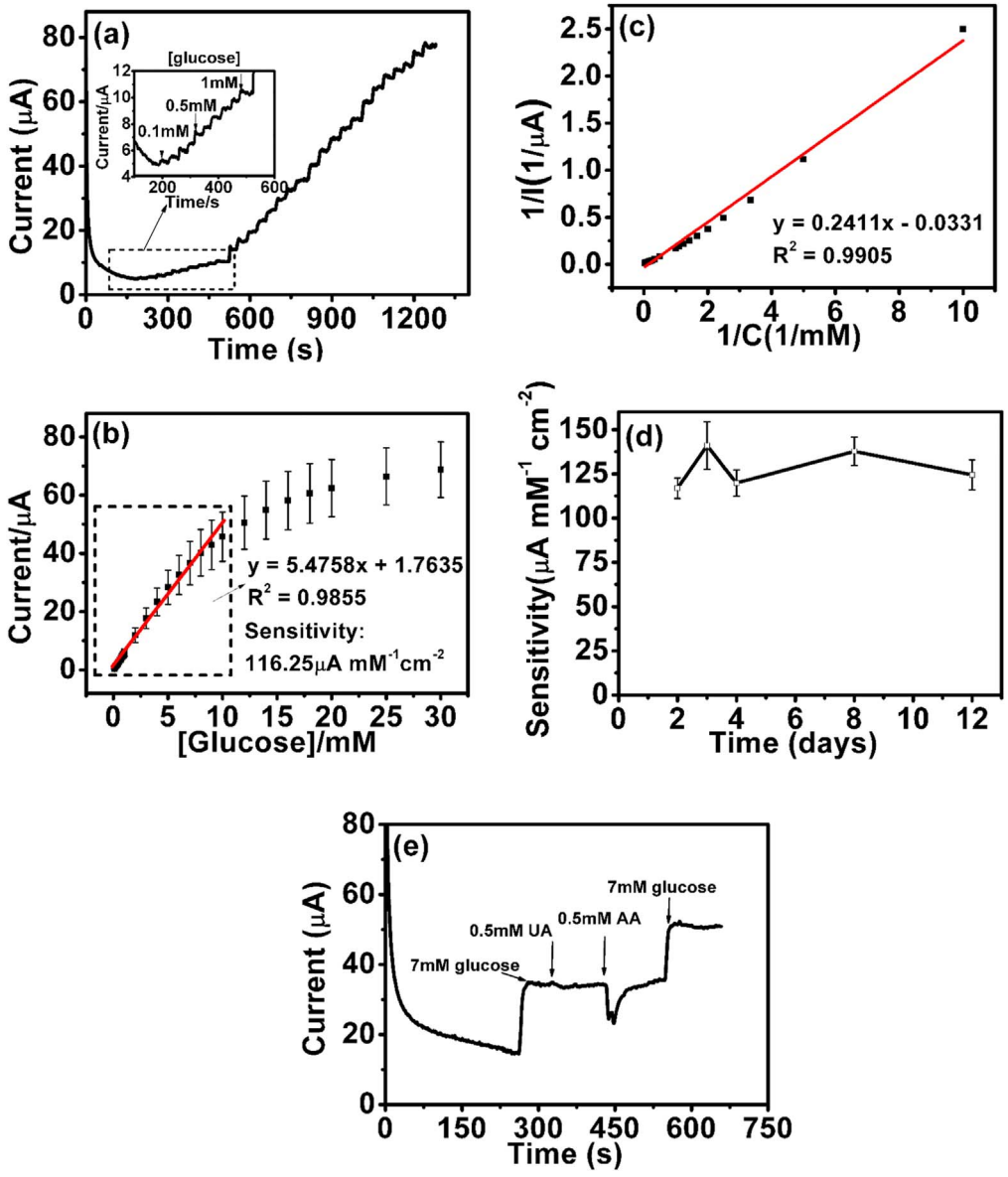

Fig. 4. Amperometric responses (a) and calibration curve (b) based on amperometric response for the sensing of glucose with Nafion/GOx-PtNPs-PEDOT-MSs SPE in 0.1 M PBS at + 0.6 V applied potential (n = 3). Insert (a) is the magnification of response current with glucose concentration from 0.1mM to 1 mM, insert (b) is the linear regression equations of response current with glucose from 0.1 to 10 mM. (c) Lineweaver-Burk plot of Nafion/GOx-PtNPs-PEDOT-MSs SPE. (d) 12 days stability test of Nafion/GOx-PtNPs-PEDOT-MSs/SPE glucose biosensor at room temperature. (e) Interference studies with uric acid (UA) and ascorbic acid (AA) in 0.01 M phosphate buffer (pH 7.4).

Table 1
Comparison of analytical performance of PEDOT-based glucose biosensors.

Electrode matrix	Linear range (mM)	Sensitivity ($\mu A\ mM^{-1}\ cm^{-2}$)	Response time (s)	Stability (days)	References
GOx/PEDOT-MSs-PtNPs/SPE	**0.1–10**	**116.25**	**5–7**	**12(97.24%)**	**This work**
PEDOT-Pd/GOx-ME	0.5–30	1.6	–	12(75%)	Santhosh et al. (2009)
PEDOT/GOx/Pt	0.1–10	12.42	4–10	18(80%)	Nien et al. (2006)
PEDOT-PSS/GOx/ITO	0–8	0.05	20	7(81%)	Park et al. (2008)
PEDOT-PSS/GOx/HRP	0.59–1.44	20.5	3	–	Yun et al. (2011)
GOx/PEDOT/PSS-PVA/Pt/ITO	0.1–1	14.06	–	–	Jung et al. (2011)
NPG/PEDOT/GOx	0.1–15	7.3	15	7(85%)	Xiao et al. (2013)
GOx/CNT/PEDOT/CFE	0.05–1.25	42	–	40(90%)	Barsan et al. (2016)
GOx/PEDOT/PMB/GCE	0.02–1.4	31.4	4	7(95%)	Kakhki et al. (2013)

responses of the Nafion/GOx-PtNPs-PEDOT-MS-based biosensors for the detection of low (0.5 mM), medium (4 mM) and high (8 mM) glucose concentration were monitored for a period of 12 days. All electrodes were maintained at a normal operating room temperature of 22 °C. The stability of the GOx-PtNPs-PEDOT-MS-based biosensors represented by the sensor sensitivity as function of time is shown in Fig. 4**d**. It clear that the GOx-PtNPs-PEDOT-MS-based biosensors were relatively stable and retained 97.24% of their average sensitivity after 12 days. The selectivity of the enzyme electrode is an important characteristic for the specific recognition of the target substrate. The selectively of the Nafion/GOx-PtNP-PEDOT-MS-based biosensors was studied by the addition of common interfering substances presence in biological sample, i.e. 0.5 mM uric acid (UA) and 0.5 mM ascorbic acid (AA) (Fig. 4**e**). The concentrations of the tested interferences were

chosen based on their respective concentrations in human serum (Safavi et al., 2006). There was no noticeable interference upon addition of UA and AA during the amperometric measurement of 7 mM glucose, likely due to the anti-interference properties of the Nafion matrix (Manesh et al., 2008).

4. Conclusions

We have demonstrated the fabrication of electrochemical biosensors using an advanced enzyme-hybrid conductive composite comprising GOx-PtNPs-PEDOT-MSs. The synthesis of the enzyme-hybrid conductive composite was based on a $CaCO_3$ template-assisted polymerisation method. The GOx-PtNP-PEDOT-MSs possess good water processability, intrinsic biocatalytic activity and conductivity thus facilitating the convenient fabrication of modified electrodes by drop casting methods. Our results showed that the GOx-PtNP-PEDOT-MS-based glucose biosensor exhibited a good sensitivity of 116.25 $\mu A\, mM^{-1}/cm^{-2}$, a limit of detection of 1.55 μM, and retained 97% of the sensitivity after 12 days storage at room temperature. A limitation of the current paper is the manual deposition of the GOx-PtNP-PEDOT-MS film, which has a relatively high surface roughness and inconsistent surface compared with electrochemically polymerised PEDOT film, and this resulted in a relatively large error between individually prepared biosensors. This would be improved by using an automatic deposition system for more precise fabrication of the biosensors. We envision that this concept could potentially be extended to other conducting polymers and biomolecules for the development of advanced functional bio-conductive inks for the convenient and easy manufacture of printed biosensors using screen-printing, ink-jet printing or drop-on-delivery systems. Machine manufacture of new biosensors is essential for their widespread introduction to the market and novel approaches to formulation of composite inks such as described here are key enablers for future success.

Acknowledgments

The authors would like to acknowledge the Swedish Research Council (VR-2015-04434) and China Scholarship Council (CSC) (File no. 201406910068) for generous financial support to carry out this research.

References

Achlioptas, D., D'Souza, R., Spencer, J., 2009. Science 323 (5920), 1453–1455.
Alemu, D., Wei, H., Ho, K., Chu, C., 2012. Energy Environ. Sci. 5, 9662–9671.
Bandodkar, A., Jeerapan, I., Wang, J., 2016. ACS Sens. 1 (5), 464–482.
Barsan, M., Pifferi, V., Falciola, L., Brett, C., 2016. Anal. Chim. Acta 927, 35–45.
Bo, X., Zhou, M., Guo, L., 2017. Biosens. Bioelectron. 89, 167–186.
Dimitriev, O., Piryatinski, Y., Pud, A., 2011. J. Phys. Chem. B 115 (6), 1357–1362.
Du, X., Zhou, C., Mai, Y., 2009. Mater. Lett. 63, 1590–1593.
Guo, Z., Qiao, Y., Liu, H., Ding, C., Zhu, Y., Wan, M., Jiang, L., 2012. J. Mater. Chem. 22 (33), 17153.
Han, M., Armes, S., 2003. Langmuir 19, 4523–4526.
Henderson, A., Saunders, J., Mrkic, J., Kent, P., Gore, J., Saunders, B., 2001. J. Mater. Chem. 11, 3037–3042.
Ishiguro, Y., Inagi, S., Fuchigami, T., 2011. Langmuir 27 (11), 7158–7162.
Jung, S., Lee, Y., Son, Y., 2011. J. Electrochem. Sci. Technol. 2 (2), 124–129.
Kakhki, S., Barsan, M., Shams, E., Brett, C., 2013. Electroanalysis 25, 77–84.
Kergoat, L., Piro, B., Simon, D., Pham, M., Noël, V., Berggren, M., 2014. Adv. Mater. 26 (32), 5658–5664.
Kros, A., Hövell, S., Sommerdijk, N., Nolte, R., 2001. Adv. Mater. 13 (20), 1555–1557.
Kumar, S., Ahlawat, W., Kumar, R., Dilbaghi, N., 2015. Biosens. Bioelectron. 70, 498–503.
Liu, J., He, K., Wu, W., Song, T., Kanatzidis, M., 2017. J. Am. Chem. Soc. 139 (8), 2900–2903.
Lu, J., Do, I., Drzal, L., Worden, R., Lee, I., 2008. ACS Nano 2 (9), 1825–1832.
Luzio, A., Musumeci, C., Newman, C., Facchetti, A., Marks, T., Pignataro, B., 2011. Chem. Mater. 23, 1061–1069.
Mak, W.C., Cheung, K.Y., Trau, D., Warsinke, A., Scheller, F., Renneberg, R., 2005. Anal. Chem. 77, 2835–2841.
Mak, W.C., Georgieva, R., Renneberg, R., Bäumler, H., 2010. Adv. Funct. Mater. 20, 4139–4144.
Manesh, K., Kim, H., Santhosh, P., Gopalan, A., Lee, K., 2008. Biosens. Bioelectron. 23, 771.
Ndamanisha, J., Guo, L., 2012. Anal. Chim. Acta 747 (20), 19–28.
Nien, P., Tung, T., Ho, K., 2006. Electroanalysis 18 (13 – 14), 1408–1415.
Nugent, J., Santhanam, K., Rubio, A., Ajayan, P., 2001. Nano Lett. 1 (2), 87–91.
Paradee, N., Sirivat, A., 2014. Polym. Int. 63, 106–113.
Park, J., Hong, K., Son, Y., 2008. Sens. Actuators B – Chem. 133 (1), 244–250.
Piro, B.T., Dang, L.A., Pham, M.C., Fabiano, S., Tran-Minh, C., 2001. J. Electroanal. Chem. 512 (1–2), 101–109.
Prakash, S., Chakrabarty, T., Singh, A., Shahi, V., 2013. Biosens. Bioelectron. 41, 43–53.
Saei, A., Najafi-Marandi, P., Abhari, A., Guardia, M., Dolatabadi, J., 2013. TrAC-Trend Anal. Chem. 42, 216–227.
Safavi, A., Maleki, N., Moradlou, O., Tajabadi, F., 2006. Anal. Biochem. 359 (2), 224–229.
Santhosh, P., Manesh, K., Uthayakumar, S., Komathi, S., Goplan, A., Lee, K., 2009. Bioelectrochemistry 75 (1), 61–66.
Sekretaryova, A., Eriksson, M., Turner, A.P.F., 2016. Biotechnol. Adv. 34, 177–197.
Simon, D., Gabrielsson, E., Tybrandt, K., Berggren, M., 2016. Chem. Rev. 116 (21), 13009–13041.
Solanki, P., Kaushik, A., Agrawal, V., Malhotra, B., 2011. NPG Asia Mater. 3 (1), 17–24.
Solomon, S., Bahadory, M., Jeyarajasingam, A., Rutkowsky, S., Boritz, C., 2007. J. Chem. Educ. 84 (2), 322.
Sukhorukov, G., Volodkin, D., Günther, A., Petrov, A., Shenoy, D., Möhwald, H., 2004. J. Mater. Chem. 14 (14), 2073–2081.
Thomas, J., Leung, K., 2014. Adv. Funct. Mater. 24, 4978–4985.
Tourillon, G., Garnier, F., 1983. J. Phys. Chem. 87, 2289–2292.
Tricoli, A., Nasiri, N., De, S., 2017. Adv. Funct. Mater. 27 (15), 1605271.
Unnikrishnan, B., Palanisamy, S., Chen, S., 2013. Biosens. Bioelectron. 39 (1), 70–75.
Vagin, M.V., Jeerapan, I., Wannapob, R., Thavarungkul, P., Kanatharana, P., Anwar, N., McCormac, T., Eriksson, M., Turner, A.P.F., Jager, E.W.H., Mak, W.C., 2016. Electrochim. Acta 190, 495–503.
Vasilevaa, N., Godjevargova, T., 2005. Mater. Sci. Eng. C – Mater. 747 (20), 19–28.
Volodkin, D., Von Klitzing, R., Mohwald, H., 2010. Angew. Chem. Int. Ed. Engl. 49 (48), 9258–9261.
Wannapob, R., Vagin, M.Y., Jeerapan, I., Mak, W.C., 2015. Langmuir 31 (43), 11904–11913.
Wannapob, R., Vagin, M.Y., Liu, Y., Thavarungkul, P., Kanatharana, P., Turner, A.P.F., Mak, W.C., 2017. ACS Appl. Mater. Interfaces. http://dx.doi.org/10.1021/acsami.7b12559.
Wu, S., Ju, H., Liu, Y., 2007. Adv. Funct. Mater. 17 (4), 585–592.
Xia, L., Wei, Z., Wan, M., 2010. J. Colloid Interface Sci. 341 (1), 1–11.
Xiao, X., Wang, M., Li, H., Si, P., 2013. Talanta 116, 1054–1059.
Xing, Z., Chang, Y., Kang, I., 2010. Sci. Technol. Adv. Mater. 11, 014101.
Yang, N., Chen, X., Ren, T., Zhang, P., Yang, D., 2015. Sens. Actuators B – Chem. 207, 690–715.
Yun, Y., Lee, B., Choi, J., Kim, S., Yoo, B., Kim, Y., Park, K., Cho, Y., 2011. Anal. Sci. 27 (4), 375.
Zhang, Y., Xin, M., Lin, W., Yu, Z., Peng, J., Xu, K., Chen, M., 2014. Synth. Met. 193, 8–16.